J|A|C|S COMMUNICATIONS

Published on Web 07/26/2010

Size Selection and Concentration of Silver Nanoparticles by Tangential Flow Ultrafiltration for SERS-Based Biosensors

John C. Trefry,[‡] Jennifer L. Monahan,[†] Kent M. Weaver,[†] Allie J. Meyerhoefer,[†] Marjorie M. Markopolous,[†] Zachary S. Arnold,[†] Dawn P. Wooley,*[,‡] and Ioana E. Pavel*[,†]

Department of Chemistry and Department of Neuroscience, Cell Biology, and Physiology, Wright State University, 3640 Colonel Glenn Highway, Dayton, Ohio 45435

Received May 4, 2010; E-mail: ioana.pavel@wright.edu; dawn.wooley@wright.edu

Abstract: A proposed tangential flow ultrafiltration method was compared to the widely used ultracentrifugation method for efficiency and efficacy in concentrating, size selecting, and minimizing the aggregation state of a silver nanoparticle (AgNP) colloid while probing the AgNPs' SERS-based sensing capabilities. The ultrafiltration method proved to be more efficient and more effective and was found to tremendously boost the SERS-based sensing capabilities of these AgNPs through the increased number of homogeneous SERS hot spots available for a biotarget molecule within a minimal focal volume. Future research studies and applications addressing the physiochemical properties or biological impact of AgNPs would greatly benefit from ultrafiltration for its ability to generate monodisperse colloidal nanoparticles, to eliminate excess toxic chemicals from nanoparticle synthesis, and to obtain minimum levels of aggregation during nanoparticle concentration.

Silver nanoparticle (AgNP) preparation and manipulation is an extremely active research area due to the numerous applications of these nanomaterials to catalysis, photonics, electronics, biosensing, drug delivery, pharmaceuticals, etc.[1] One of the most exciting and demanding applications of AgNPs is their surface-enhanced Raman spectroscopy (SERS)-based biosensing capabilities. SERS is a powerful analytical technique, which has experienced an explosive interest due to its strong molecular specificity and its extremely low detection limits, down to the single-molecule level.[2a,b] Theory predicts[2c,d] and experiments confirm[2a,b,1c] that exceptionally large increases in a Raman cross section are associated with molecules located in the nanosized interstitial sites of interacting colloidal AgNPs (i.e., hot spots).

Significant challenges remain for the preparation and isolation of colloidal AgNPs with controlled polydispersity, toxicity, and aggregation.[3] Limiting AgNP polydispersity (i.e., narrow size and shape distribution)[3a] improves the optical/electronic properties,[2c,d,3a] SERS enhancement factors,[2c,d] and antimicrobial properties.[1e,3f] Reducing AgNP toxicity by eliminating chemically aggressive reagents or organic solvents[3a,c] significantly lowers the impact to biological systems, while facilitating the identification of novel activities and mechanisms.[1e,3c−e] Minimizing AgNP aggregation at higher concentrations[1c,3a,c] allows the assessment of the SERS nanostructure−function relationship,[2c,d] improves the cellular uptake of AgNPs,[1c,3d−f] and maintains the number of potentially active catalytic sites.[1a] Additionally, use of methods such as centrifugation,[4a] size exclusion chromatography,[4a,b] gel electrophoresis,[4c] diafiltration,[4d] size-dependent solubility,[4e] and fractional crystallization[4f] have been reported for the size-based separation and/or concentration of NPs. These approaches may lead to issues with aggregation,[4a] instability,[4a] cost,[4b,e] undesired coatings,[4c,f] and less effective protocols for NPs of smaller size.[4f] As a result, these methods are time intensive, expensive, toxic, or inefficient.[4] These limitations were overcome in this study by using a tangential flow ultrafiltration method, commonly used for weight-based separation of proteins but not yet tested on silver or polydisperse colloids.[4d] Tangential flow ultrafiltration is a single pass procedure to size select and to concentrate a target species using a series of membrane modules with pores ranging from 1 nm to 100 μm. The proposed method was compared to the widely used ultracentrifugation method for efficiency and efficacy in concentrating, size selecting, and minimizing the aggregation state of an AgNP colloid while probing the AgNPs' SERS-based sensing capabilities.

Colloidal AgNPs were synthesized according to a well-known, inexpensive Creighton method by the simple reduction of silver nitrate with sodium borohydride. Once synthesized, the 600 mL original colloid (Ori) product was divided into two aliquots for the comparative analysis. Ultracentrifugation was performed at 7.8×10^3 *g* and 10 °C for 90 min to separate the colloid into a supernatant (Csu) and a pellet (Cpl) of AgNPs. Cpl was resuspended in 10 mL of supernatant. For ultrafiltration, the colloid was pumped through a 50 nm filter yielding a concentrate (50c; AgNPs > pore size) and a filtrate (50f; AgNPs < pore size) sample. The 50f sample was then pumped through a 100 kD filter to produce a concentrated (100c) sample (Figure S1).

Visual inspection, transmission electron microscopy (TEM), UV−vis absorption, and flame atomic absorption spectrophotometry (FAAS) measurements on each sample revealed corroborating data that the ultrafiltration method was more efficient at specific size selection and concentration of AgNPs with minimal aggregation than ultracentrifugation (Figure 1A, Table 1). The dramatic color change between Ori, Cpl, and 100c confirms that darker, more opaque solutions contain larger particles with high levels of AgNP aggregation (Figure 1A, column 1).[5a] TEM micrographs (Figure 1A, column 1) show that Ori is characteristic of moderately dispersed, lowly concentrated AgNPs. Cpl contains high concentra-

Table 1. Specific Characteristics of Each AgNP Preparation[a]

Sample	Ori	Csu	Cpl	50c	50f	100c
Ave.	10.4	8.5	11.4	18.2	3.3	11
Max.	141	54.4	161	162.5	87.3	60.5
%Dist.	100	106	162	129	127	73
Conc.	15.3	7.9	77.4	16.4	14.3	198.7

[a] Average size in nm (Ave.), maximum size in nm (Max.), percent distribution (% Dist.), final concentration of silver in μg mL^{-1} (Conc.).

[†] Department of Chemistry.
[‡] Department of Neuroscience, Cell Biology, and Physiology.

10.1021/ja103809c

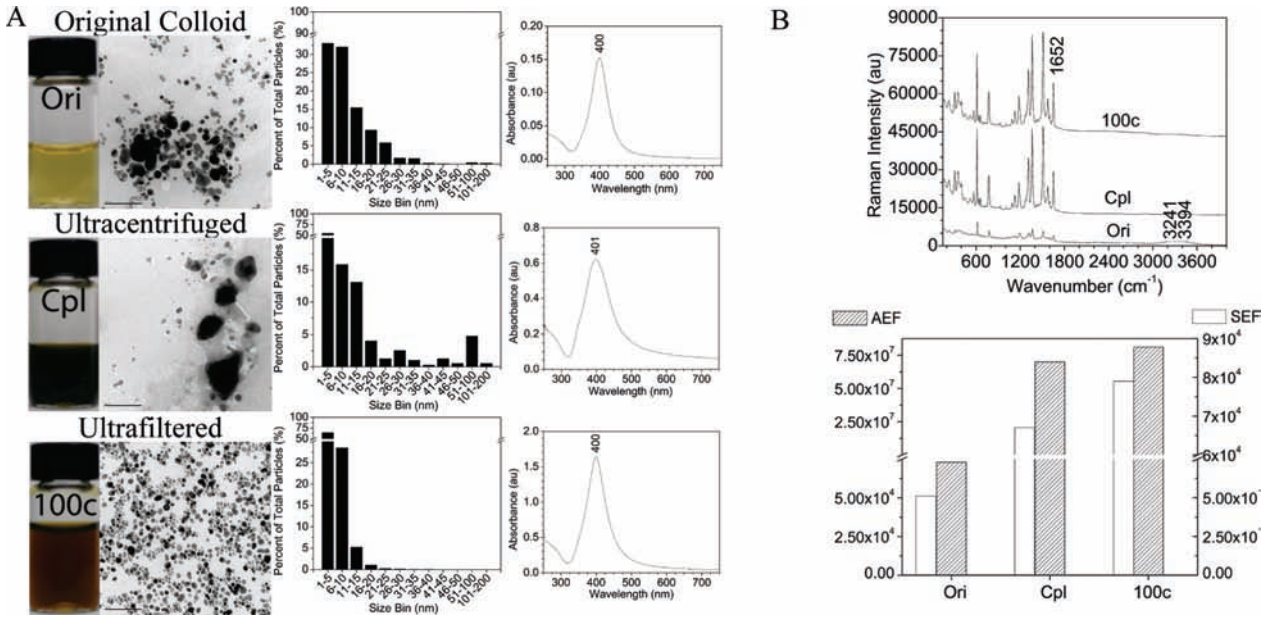

Figure 1. AgNPs were characterized at each step in the isolation and concentration process. A) Each row represents a distinct preparation: column 1) visual and TEM inspection photos, bar =100 nm, column 2) size analysis from TEM data, and column 3) UV−vis absorption spectra. B top) SERS spectra of R6G dye (10^{-6} M) on each colloid excited at 632.8 nm. B bottom) Estimated analytical (AEF) and surface enhancement factors (SEF) for each colloid.

tions of massive, heterogeneous AgNP aggregates. 100c consists of highly concentrated yet lowly aggregated and homogeneous AgNPs. The UV−vis spectra show both Ori and 100c samples had surface plasmon resonance (SPR) absorption maxima at 400 nm but 100c had a 10-fold higher intensity. This sharp, symmetrical peak is characteristic of small (10−20 nm diameter) and spherical AgNPs of low aggregation.[5b] The spectra for Cpl had a broader SPR peak with a clear shoulder, showing the ultracentrifugation process leads to the formation of polydisperse AgNP aggregrates.

Size histograms (Figure 1A, column 2) were prepared by analyzing the TEM micrographs of each sample (number of AgNPs = 500). The differences in size distribution and maximum diameters for the Ori and Cpl samples compared to the 100c sample are significant (e.g., more than twice for Cpl). Most of the aggregates larger than 20 nm were eliminated in 100c (Figure 1, column 2), while Cpl had increased numbers of larger aggregates (5% of the total AgNPs have diameters 50 nm or larger). These large aggregates produced by ultracentrifugation accounted for 96% of the AgNP weight. Ultrafiltration was also 2.5-fold more efficient at concentrating the Ori colloid (from 77.4 to 198.7 μg mL^{-1} of silver). Concentration factors for Cpl and 100c were 5.1- and 13.0-fold, respectively (Table 1).

The SERS-sensing efficiencies, the analytical (AEF) and surface enhancement factors (SEF), of Ori, Cpl, and 100c were calculated by measuring the Raman, SERS, and fluorescence spectra of a 10^{-6} M rhodamine 6G (R6G) solution as a standard (Figure 1B; Supporting Information).[5b,c] The enhancement factors for Cpl and 100c were found to have similar values (e.g., AEF of 8.1×10^7 and SEF of 7.9×10^4 for 100c). These factors are 1000-fold larger than those calculated for Ori. Recent studies[5c] showed that a SEF of 10^7 is sufficient to observe single-molecule SERS events for an R6G concentration of 10^{-9} M, at 632.8 nm, and with an integration time of 1 s. The fluorescence data indicate that 100c and Cpl have comparable, improved R6G absorption abilities. Over 96% of the R6G molecules effectively complexed to the AgNP surface and contribute to the SERS signal in 100c and Cpl (70% of the R6G probes for Ori). The enormous increase in signal for 100c is due to the highly concentrated, uniform colloidal AgNPs available for creating dimers or small AgNP aggregates. Although the amount of silver is 2.5-fold less in Cpl, similar enhancement factors are achieved due to the large, heterogeneous AgNP aggregates. However, the Cpl aggregates are formed in an uncontrolled manner and may impede cellular uptake and assessment of the nanostructure−function relationship.

The data presented here demonstrate that ultrafiltration permits greater control over AgNP size, concentration, and aggregation state than conventional methods of isolation such as ultracentrifugation. Future research studies and applications addressing the physiochemical properties or biological impact of AgNPs would greatly benefit from ultrafiltration for its ability to generate monodisperse colloidal NPs, to eliminate excess toxic chemicals from NP synthesis, and to obtain minimum levels of aggregation during NP concentration. The ultrafiltration method for AgNP isolation could tremendously boost the SERS-based sensing capabilities of these nanomaterials through the increased number of homogeneous SERS hot spots available for a biotarget molecule within a minimal focal volume. Additionally, ultrafiltration could easily be implemented at various volume scales, for both research and industrial purposes.

Acknowledgment. We thank Dr. Gerald M. Alter for the use of the fluorescence spectrophotometer in his research laboratory. I.E.P. gratefully acknowledges the WSU Women in Science Giving Circle Award.

Supporting Information Available: Experimental methods and AEF/SEF calculations. This material is available free of charge via the Internet at http://pubs.acs.org.

References

(1) (a) Jana, N. R.; Sau, T. K.; Pal, T. *J. Phys. Chem. B* **1999**, *103*, 115–121. (b) Li, Y.; Wu, Y.; Ong, B. S. *J. Am. Chem. Soc.* **2005**, *127*, 3266–3267. (c) Willets, K. A. *Anal. Bioanal. Chem.* **2009**, *394*, 85–94. (d) Jain, J.; Arora, S.; Rajwade, J. M.; Omray, P.; Khandelwal, S.; Paknikar, K. M. *Mol. Pharm.* **2009**, *6*, 1388–1401. (e) Bhattacharya, R.; Mukherjee, P. *Adv. Drug. Delivery Rev.* **2008**, *60*, 1289–1306.

(2) (a) Nie, S.; Emory, S. R. *Science* **1997**, *275*, 1102–1106. (b) Xu, H.; Bjerneld, E. J.; Käll, M.; Börjesson, L. *Phys. Rev. Lett.* **1999**, *83*, 4357–4360. (c) Xu, H.; Aizpurua, J.; Käll, M.; Apell, P. *Phys. Rev. E* **2000**, *62*, 4318–4324. (d) Aravind, P. K.; Nitzan, A.; Metiu, H. *Surf. Sci.* **1981**, *110*, 189–204.

(3) (a) Sun, Y.; Xia, Y. *Science* **2002**, *298*, 2176–2179. (b) Jana, N. R.; Peng, X. G. *J. Am. Chem. Soc.* **2003**, *125*, 14280–14281. (c) Tolaymat, T. M.; El Badawy, A. M.; Genaidy, A.; Scheckel, K. G.; Luxton, T. P.; Suidan, M. *Sci. Total Environ.* **2010**, *408*, 999–1006. (d) Miura, N.; Shinohara, Y. *Biochem. Biophys. Res. Commun.* **2009**, *390*, 733–737. (e) Auffan, M.; Rose, J.; Bottero, J.-Y.; Lowry, G. V.; Jolivet, J.-P.; Wiesner, M. R. *Nat. Nanotechnol.* **2009**, *4*, 634–641. (f) AshaRani, P. V.; Mun, G. L. K.; Hande, M. P.; Valiyaveettil, S. *ACS Nano* **2009**, *3*, 279–290. (g) Scown, T. M.; Santos, E. M.; Johnston, B. M.; Gaiser, N.; Baalousha, M.; Mitov, S.; Lead, J. R.; Stone, V.; Fernandes, T. S.; Jepson, M.; van Aerle, R.; Tyler, C. R. *Toxicol. Sci.* **2010**, *115*, 521–534.

(4) (a) Novak, J. P.; Nickerson, C.; Franzen, S.; Feldheim, D. L. *Anal. Chem.* **2001**, *73*, 5758–5761. (b) Al-Somali, A. M.; Krueger, K. M.; Falkner, J. C.; Colvin, V. L. *Anal. Chem.* **2004**, *76*, 5903–5910. (c) Hanauer, M.; Pierrat, S.; Zins, I.; Lotz, A.; Sönnichsen, C. *Nano Lett.* **2007**, *7*, 2881–2885. (d) Sweeny, S. F.; Woehrle, G. H.; Hutchison, J. E. *J. Am. Chem. Soc.* **2006**, *128*, 3190–3197. (e) Clarke, N. Z.; Waters, C.; Johnson, K. A.; Satherley, J.; Schiffrin, D. J. *Langmuir* **2001**, *17*, 6048–6050. (f) Schaaff, T. G.; Shafigullin, M. N.; Khoury, J. T.; Vezmar, I.; Whetten, R. L.; Cullen, W. G.; First, P. N. *J. Phys. Chem. B* **1997**, *101*, 7885–7891.

(5) (a) Sönnichsen, C.; Reinhard, B. M.; Liphardt, J.; Alivisatos, A. P. *Nat. Biotechnol.* **2005**, *23*, 741–745. (b) Ciou, S. H.; Cao, Y. W.; Huang, H. C.; Su, D. Y.; Huang, C. L. *J. Phys. Chem. C* **2009**, *113*, 9529–9525. (c) Le Ru, E. C.; Blackie, E.; Meyer, M.; Etchegoin, P. G. *J. Phys. Chem. C* **2007**, *111*, 13794–13803.

JA103809C